Sequence Decoding of 1D to 2D Self-Assembling Cyclic Peptides

Sandra Díaz, Ignacio Insua, Ghibom Bhak, Javier Montenegro

FULL PAPER

Sequence Decoding of 1D to 2D Self-Assembling Cyclic Peptides

Sandra Díaz[+], Ignacio Insua[+], Ghibom Bhak and Javier Montenegro*

[*] S. Díaz, Dr. I. Insua, Dr. G. Bhak and Dr. J. Montenegro
Centro Singular de Investigación en Química Biolóxica e Materiais Moleculares (CIQUS), Departamento de Química Orgánica
Universidade de Santiago de Compostela
Santiago de Compostela, 15782, Spain
E-mail: javier.montenegro@usc.es
[+] These authors contributed equally to this work.

Supporting information for this article is given via a link at the end of the document.

Abstract: The inherent ability of peptides to self-assemble with directional and rationally predictable interactions has fostered a plethora of synthetic two-dimensional (2D) supramolecular biomaterials. However, the design of peptides with hierarchical assembly in different dimensions across mesoscopic lengths remains a challenging task. We here describe the structural exploration of a D/L-alternating cyclic octapeptide capable of assembling one-dimensional (1D) nanotubes in water, which subsequently pack laterally to form giant 2D nanosheets up to 500 μm long with a constant 3.2 nm thickness. Specific amino acid mutations allowed the mapping of structure-assembly relationships that determine 2D self-assembly. Nine peptide modifications were studied, revealing key features in the peptide sequence that nanosheets tolerated, while a total of three peptide variants included modifications that compromised their 2D arrangement. These lessons will serve as guide and inspiration for new 2D supramolecular peptide designs.

Introduction

Two-dimensional (2D) self-assembly is currently attracting great attention as a versatile platform to access new responsive materials with high surface-to-volume ratios.[1–5] A wide variety of organic scaffolds have been assembled in 2D by means of all sorts of supramolecular interactions: from host-guest chemistry,[6–9] to metal complexation,[10] electrostatic forces[11–13] and orthogonal polar and hydrophobic interactions.[14–16] Supramolecular 2D materials display structural adaptability based on their reversible non-covalent bonds, thus allowing controlled dynamic polymorphism.[17–19] On the other hand, covalent 2D materials provide higher structural robustness at the expense of supramolecular responsiveness,[20,21] leading to highly porous covalent organic frameworks of high crystallinity.[22,23] However, biological compatibility can hamper the translation of these artificial 2D structures to medical devices and new-generation nanomaterials.

Natural biomolecules, primarily lipids, are present in cells as supramolecular 2D membranes that regulate important cellular functions, such as communication and cell division.[24] Non-canonical biomolecular 2D assemblies (*i.e.* not based on lipids) can be obtained through DNA origami with remarkable shape control.[25] Alternatively, peptides display spatially organised and well understood supramolecular interactions from their backbones and side chains for inter- and intramolecular self-assembly in water.[26–28] Synthetic designs capitalise on known natural peptide motifs to access new supramolecular architectures and applications,[29] for example, catalytic nanotubular ensembles,[30] cell-targeted drug nanovehicles,[31] fuelled dissipative fibrillators,[32] ultra-highly stable protein nanostructures[33] and artificial molecular transporters.[34] These developments provide valuable insight for the design and understanding of supramolecular peptide assemblies and derived applications.[24,29]

Amphiphilic peptides with segregated polar and apolar faces have been assembled in 2D membranes of very different internal structure.[35,36] These systems range from short peptide amphiphiles,[37] to oligoproline weaves,[38] trimeric peptide helices,[39] protein-metal networks[40] and non-natural peptoids,[41] amongst others. Important supramolecular learnings can be derived from this wide variety of non-covalent 2D peptide assemblies. For example, specific residue solvation was proven to control supramolecular elongation in 1D or 2D.[42] The Conticello group introduced the concept of geometrically frustrated self-assembled peptides,[43,44] where minor structural modifications in the monomeric units can induce local deformations that propagate through the network allowing predictive and size-controlled nanofabrication.[45,46] Applications of peptide-based 2D materials range from molecular recognition and binding[47] to artificial membranes,[48] scaffolds for cell growth[49] and self-replicative polymerase mimics.[50]

Despite the development of non-canonical 2D peptide membranes, the polymorphic and multidimensional self-assembly of peptides along micrometric length scales remains challenging. Understanding the design principles behind such hierarchical organisation could open access to new multifunctional and adaptive supramolecular 2D materials. Examples of multidimensional peptide assembly include amphiphilic peptides that sequentially form 1D fibrils via β-sheet interactions, which then oligomerise in 2D through lateral side chain interactions.[51,52] Likewise, β-amyloid peptides can undergo sequential multidimensional self-assembly in acidic media, transitioning from 1D fibres to 2D nanosheets that eventually coil up into 1D nanotubular scrolls.[53] However, many of these systems are based on natural peptide structures and folding motifs, making non-natural peptide analogues necessary to expand the architectures and applications accessible with supramolecular 2D materials.

Cyclic peptides with alternating D/L amino acids are artificial structures known to self-assemble in aqueous media as 1D

nanotubes via inter-backbone H-bonding.[54] Thus, flat peptide rings undergo supramolecular polymerisation into nanotubes stabilised by longitudinal β-sheet networks,[55] with amino acid side chains projected from the surface of the tubes.[56] Cyclic peptide nanotubes find application as artificial membrane transporters,[57] minimal models of natural protein organisation,[58,59] and their polymer conjugates have been studied for drug delivery.[60,61]

Beyond 1D self-assembly, our group has recently reported an amphiphilic cyclic peptide (**CP$_x$**) capable of forming nanotubes that subsequently pack in 2D to give giant supramolecular nanosheets with micrometric dimensions (**Table 1**).[62] Design-wise, the octapeptide **CP$_x$** consists of a hydrophobic tripeptide (Leu-Trp-Leu) that drives the bilayer packing of nanotubes in water, while also leucine zippers established between adjacent tubes provide directionality in the 2D elongation. The remaining residues of **CP$_x$** provide a polar anionic corona that maintains nanosheets extended and prevents supramolecular collapse. Despite this basic structural understanding, the sequence-assembly relationships of multidimensional self-assembling cyclic peptides remains to be discovered to unlock their full potential. Here, we report a systematic structural modification at key positions of **CP$_x$** to assess their effect on 2D nanosheet assembly. The amino acid mutations carried by these peptide variants provide valuable information in the hydrophilic and hydrophobic domains of the 2D assemblies to guide future supramolecular peptide designs and materials.

Results and Discussion

Structural derivatives of the original nanosheet-forming cyclic peptide **CP$_x$**[62] were designed targeting three key positions to screen structure-assembly relationships (**Table 1**). Firstly, the central hydrophobic residue in the parent structure, tryptophan, was replaced for other non-polar amino acids, spanning from non-aromatic (alanine, **CP$_A$**, and leucine, **CP$_L$**) to a less bulky aromatic residue (phenylalanine, **CP$_F$**). Secondly, the hydrophobic leucines that mediate 2D assembly via lateral association of 1D nanotubes were replaced for aromatic phenylalanines (**CP$_{2F}$**). Substitution of all three hydrophobic residues (*i.e.* leucines and tryptophan) for phenylalanines (**CP$_{3F}$**) was also explored to remove structural differences between the centre and sides of the peptide's hydrophobic face. Finally, the polar face of the peptide bearing orthogonally arranged histidine and glutamic acid residues was altered: **CP$_{oE}$** loses the frontal mismatch of histidines and glutamics, while **CP$_{2E2H}$** segregates these residues into two homodimeric domains. Also in this polar region, replacement of histidines for more basic lysines (**CP$_K$**) and a fully anionic variant with four glutamic acids (**CP$_{4E}$**) completed the library explored. Glutamine's position (R_8) was kept constant throughout the library of CPs tested for being the common anchoring point of the peptides to their solid support during synthesis, which being neutral and hydrophilic, it should not interfere with our peptide structure-assembly study. Cyclic peptides were synthesised on solid phase using conventional Fmoc chemistry and orthogonal O-allyl protecting group at the *C*-terminus for cyclisation (see Supporting Information).

Table 1. Chemical structures of all cyclic peptides covered in this study and depiction of their sequential self-assembly in one-dimensional (1D) nanotubes and two-dimensional (2D) nanosheets. Nanotubes consist of cyclic peptides stacked via hydrogen bonds (dashed lines), while nanosheets form by lateral association of tubes as leucine zippers (yellow connectors).

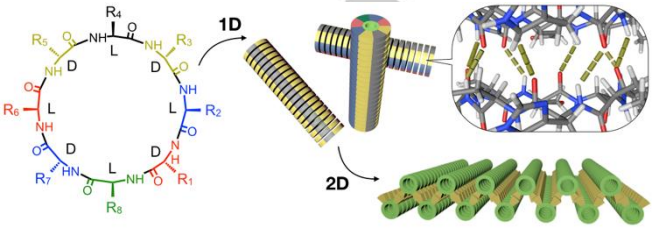

Peptide	R_1	R_2	R_3	R_4	R_5	R_6	R_7	R_8	2D[b]
CP$_x$[a]	Glu	His	Leu	Trp	Leu	Glu	His	Gln	*yes*
CP$_A$	Glu	His	Leu	**Ala**	Leu	Glu	His	Gln	*yes*
CP$_L$	Glu	His	Leu	**Leu**	Leu	Glu	His	Gln	*yes*
CP$_F$	Glu	His	Leu	**Phe**	Leu	Glu	His	Gln	*yes*
CP$_{2F}$	Glu	His	**Phe**	Trp	**Phe**	Glu	His	Gln	*yes*
CP$_{3F}$	Glu	His	**Phe**	**Phe**	**Phe**	Glu	His	Gln	*yes*
CP$_{oE}$	Glu	His	Leu	Trp	Leu	**His**	**Glu**	Gln	*yes*
CP$_{2E2H}$	**His**	His	Leu	Trp	Leu	Glu	**Glu**	Gln	*no*
CP$_K$	Glu	**Lys**	Leu	Trp	Leu	Glu	**Lys**	Gln	*no*
CP$_{4E}$	Glu	**Glu**	Leu	Trp	Leu	Glu	**Glu**	Gln	*no*

[a] Original peptide structure from previous work: amino acid mutations from this parent structure are highlighted in bold.[62] [b] Does the peptide form 2D nanosheets? See **Figure 1**.

To study nanosheet formation, all new cyclic peptides were dissolved in 20 mM sodium phosphate buffer at pH 7.4 and solutions were temperature-annealed as reported previously:[62] i) 80ºC/1.5 h; ii) room temperature/1 h. This process provides thermodynamic control over the stepwise 1D-to-2D assembly of nanosheets, as 1D nanotubes are the only supramolecular ensemble present at 80ºC, which then associate in 2D upon cooling at room temperature. All samples inspected by epifluorescence microscopy contained thioflavin-T, a fluorescent strain-sensitive probe that planarizes in hydrophobic pockets within the assembly, resulting in enhanced green fluorescence and thus reporting on supramolecular morphology.[63] Microscopic inspection of these samples revealed 2D nanosheets in six of the nine new peptide designs explored (**Figure 1**).

Mutation of the central hydrophobic residue tryptophan in the original peptide was surprisingly well tolerated. In this position, a much smaller alanine residue (**CP$_A$**) and non-aromatic leucine (**CP$_L$**) led to the formation of large micrometric nanosheets (**Figure 1**). Even the analogue **CP$_F$**, bearing an aromatic phenylalanine residue instead of tryptophan, assembled in 2D. Regarding mutations of the two original leucine residues in positions R_3 and R_5 (**Table 1**), it was previously demonstrated that an analogue bearing smaller and less hydrophobic alanine residues instead of leucine lost most of its 2D assembling capacity, forming fibrillar structures with a few small sheets.[62] Based on this result, a more hydrophobic and aromatic residue was

explored, phenylalanine, which should establish alternative phenylalanine stacks to drive the 2D arrangement of the tubes (**CP$_{2F}$**). Microscopic analysis of **CP$_{2F}$** showed well defined and extended nanosheets, demonstrating the tolerance of this key position for 2D assembly to be replaced for other hydrophobic residues (**Figure 1**). Motivated by the positive results obtained with both **CP$_{2F}$** and **CP$_{F}$** (*vide supra*), a variant with all three hydrophobic positions ($R_{3\text{-}5}$, **Table 1**) incorporating phenylalanine residues was investigated, **CP$_{3F}$**. Remarkably, the longest nanosheets across the collection of peptides presented here were found in samples of **CP$_{3F}$**, reaching over 500 µm in length, approximately twice as long as the largest nanosheets previously found for the parent peptide **CP$_{x}$** (*ca*. 260 µm).[62] However, **CP$_{3F}$** also showed background peptide aggregates in nanosheet samples, suggesting a certain degree of disordered hydrophobic packing (**Figure 1**). Same as **CP$_{L}$**, with all three hydrophobic positions filled with the same leucine residue, **CP$_{3F}$** does not segregate different amino acids in the hydrophobic tripeptide domain (**Table 1**). This lack of hydrophobic mismatch between side and central non-polar residues might compromise the lateral association of tubes via leucine or phenylalanine zippers specifically between residues R_3 and R_5. Therefore, the high degree of wrinkling of **CP$_{L}$** and **CP$_{3F}$** nanosheets, together with the background aggregation of the latter, may result from the interference of the central hydrophobic residue in the 2D elongation.

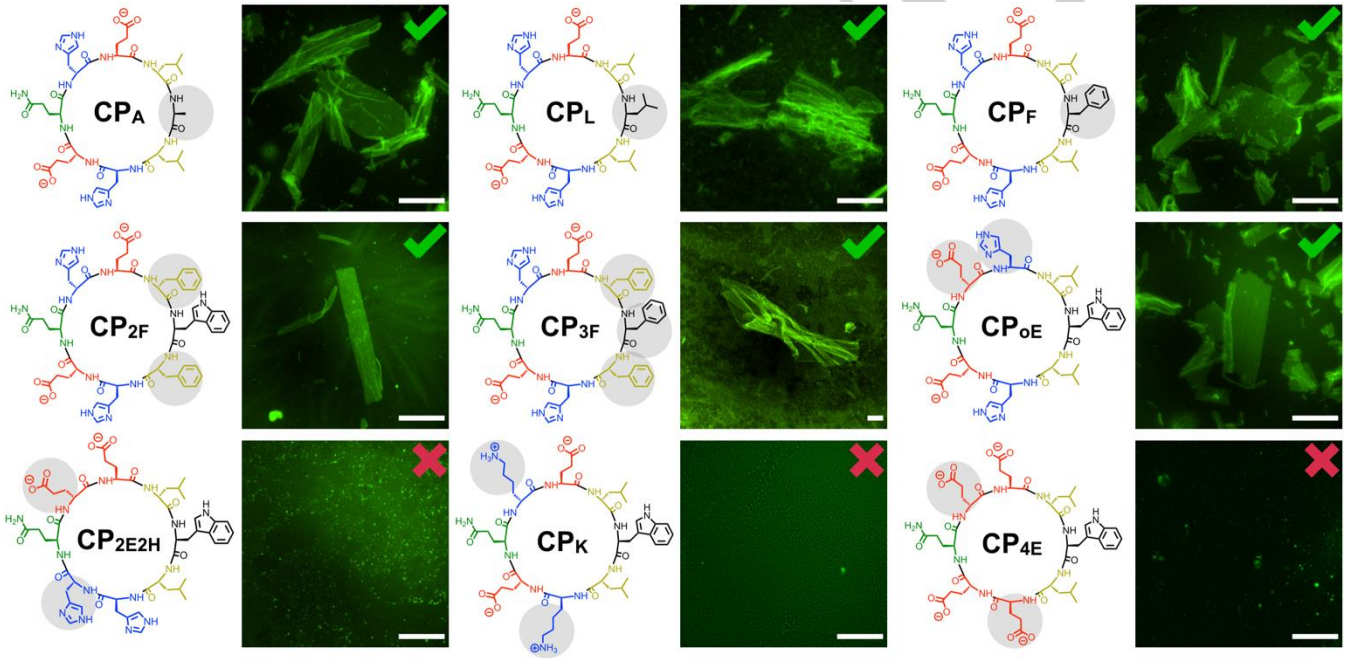

Figure 1. Chemical structures and epifluorescence micrographs of cyclic peptides (50 µM, pH 7.4) annealed for 2D self-assembly (i. 80ºC/1.5 h; ii. room temperature/1 h) in presence of thioflavin-T (10 µM). Green ticks and red crosses indicate the ability or inability of peptides to assemble 2D nanosheets, respectively. Modified amino acids from the original **CP$_{x}$** structure are highlighted over a grey background. Scale bars = 50 µm.

While the hydrophobic region of the cyclic peptides showed substantial structural flexibility, variations in the polar ionic region of the parent peptide, consisting of alternating glutamic acid and histidine residues (*i.e.* positions $R_{1\text{-}2}$ and $R_{6\text{-}7}$, **Table 1**), revealed important design requirements for nanosheet assembly. **CP$_{oE}$**, which stands for outer glutamic acids, has symmetrically distributed ionic domains unlike the original mismatched design of **CP$_{x}$**. **CP$_{oE}$** formed well defined nanosheets regardless of this sequence alteration. However, segregation of glutamic acid and histidine residues on two opposite sides of the peptide completely inhibited nanosheet formation (**CP$_{2E2H}$**, **Figure 1**). These results indicate that, despite allowing order variations, glutamic acid and basic histidine residues must be placed together in the peptide sequence. This requirement is probably due to the weakening of like-charge repulsions from glutamic carboxylates by partially protonated histidines (pK_a~6.0).

Substitution of histidines in the parent peptide for more basic lysine residues (pK_a~10.6) was also explored to assess the ability of a fully ionized peptide with zero net charge to assemble nanosheets. Unfortunately, **CP$_{K}$** did not form nanosheets (**Figure 1**), indicating that a certain repulsive character is required for cyclic peptides to assemble in 2D. Being charge repulsions necessary for self-assembly, a derivative with four anionic glutamic acids was evaluated. However, **CP$_{4E}$** was also unable to assemble nanosheets, probably as a result of very high energy barriers derived from this more self-repulsive and strongly anionic structure (**Figure 1**).

It has been shown that cyclic peptide self-assembly can be triggered by pH and ionic strength[58,59,62] as a means to balance the electrostatic forces between peptide monomers. Hence, we also tested the formation of nanosheets with cyclic peptides unable to assemble in 2D under the general conditions used here (*i.e.* 20 mM sodium phosphate buffer at pH 7.4) at different pH

and NaCl concentrations. **CP$_{2E2H}$**, was unable to form nanosheets at neither pH 7.4, 4.0 nor 2.0, as the peptide's net change transitions from fully anionic to fully cationic (**Figure S19**). Interestingly, **CP$_{4E}$** showed very small platelets (3.7±0.4 µm; *n*=20) at pH 4.0, which matches glutamic acid's pK_a, that could arise form a 1:1 equilibrium between repulsive anionic and attractive neutral ionisation states (**Figure S20**). These platelets disappeared at pH 2.0, where no electrostatic repulsion between fully neutral **CP$_{4E}$** units exists. With regards to electrostatic shielding by salts, addition of NaCl up to a concentration of 100 mM did not trigger nanosheet formation with neither **CP$_{2E2H}$** nor **CP$_{4E}$** (**Figures S21-22**). Overall, these results confirm the stronger sequence dependence of amphiphilic cyclic peptides for sequential 1D and 2D self-assembly over external stimuli such as pH and ionic strength.

Microscopic analysis of the new peptide assemblies was performed to confirm the structural analogy with the original **CP$_x$** nanosheets, consisting of laterally bound nanotubes forming a staggered bilayer (**Table 1**). **CP$_A$** was selected as a representative peptide across the collection, showcasing an important reduction in bulkiness and hydrophobicity from the original tryptophan position. Additionally, **CP$_A$** lacks the π-π stacking and H-bonding capacity of the parent **CP$_x$** as a result of this single amino acid replacement. Scanning-transmission electron microscopy (STEM) of **CP$_A$** nanosheets showed homogeneous film surfaces with localized signs of tearing, where the backward 2D to 1D disassembly of the system revealed laterally associated nanotubes (**Figure 2A-B**). This continuous transition between 2D and 1D states along the same nanosheet was previously observed in the original **CP$_x$**,[62] and it confirms the nanotubular composition of the new 2D assemblies. As expected, the corresponding atomic force microscopy (AFM) of **CP$_A$** nanosheets showed heights between 3.1 and 3.3 nm, which were consistent with the 3.2 nm height previously found in **CP$_x$** nanosheets (**Figure 2C-D**). Hence, STEM and AFM analysis confirmed the nanotubular bilayer structure of the nanosheets obtained from the cyclic peptides investigated in this study (**Table 1**), identical to the supramolecular architecture found in the original **CP$_x$** nanosheets.[62]

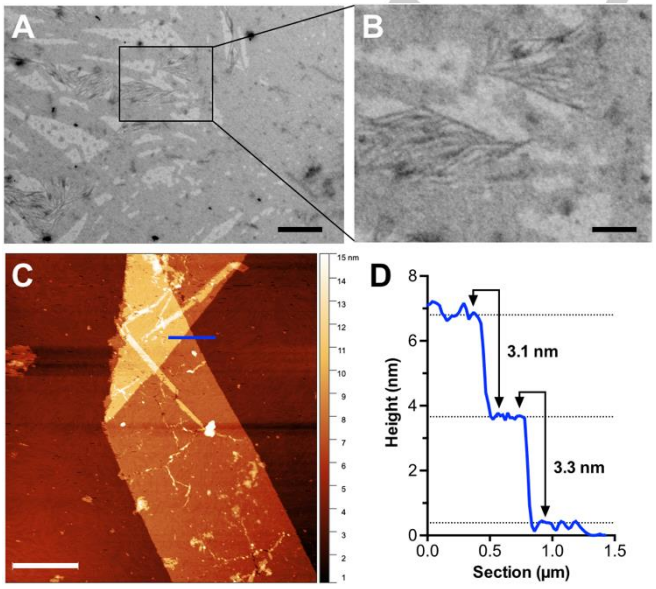

Figure 2. STEM (A-B) and AFM (C) images of **CP$_A$** nanosheets. (D) AFM Z-height profile of the blue section across a folded nanosheet. Scale bars: 300 nm (A), 100 nm (B) and 2 µm (C).

Conclusion

In this paper we describe the systematic structural exploration of an octameric D/L-alternating cyclic peptide capable of sequential self-assembly in aqueous medium in 1D and 2D. Three key positions in this parent octapeptide sequence (**CP$_x$**) were targeted: its central hydrophobic group, the two lateral hydrophobic amino acids responsible for 2D growth, and the acidic and basic residues that establish the polar shell of the final assembly. From the nine new peptide structures presented here, six of them could form 2D nanosheets (**Figure 1**). Overall, modifications in the central hydrophobic position, originally occupied by tryptophan, were very well tolerated, with alanine (**CP$_A$**), leucine (**CP$_L$**) and phenylalanine (**CP$_F$**) showing 2D assembly. Replacement of leucine residues as nanotubular side connectors for phenylalanine zippers preserved the lateral connectivity and 2D assembling capacity of the parent peptide (**CP$_{2F}$** and **CP$_{3F}$**). It was also demonstrated that ionizable glutamic and histidine residues must be placed together in the peptide sequence regardless of their order (**CP$_{oE}$**), but never segregated on different sides of the peptide (**CP$_{2E2H}$**). Peptides with no electrostatic repulsion (**CP$_K$**) or with a very strong one (**CP$_{4E}$**) did not form nanosheets, lacking for either reason the balanced repulsive component required to extend the mesoscopic 2D structure of these nanosheets. Finally, STEM and AFM analysis demonstrated the internal structure of these supramolecular 2D nanosheets as bilayers of laterally arrayed 1D nanotubes, analogous to the original **CP$_x$**, thus proving the tolerance of this 2D system to certain amino acid alterations. Overall, these results provide important design rules for the self-assembly of peptides - not only cyclic sequences- and derivatives thereof (*e.g.* peptoids and non-peptide conjugates) in aqueous solution, with future potential application in biomaterial design, nanotechnology, medicine and cellular engineering.

Experimental Section

Nanosheet annealing. Cyclic peptides were dissolved to a concentration of 50 µM in sodium phosphate buffer (20 mM, pH 7.4) and solutions were sonicated for 5 min. Then, samples were incubated without shaking at 80ºC for 1.5 h. Next, peptide solutions were stored at room temperature for 1 h, where 2D elongation takes place. For nanosheet formation at a different pH or in presence of NaCl, cyclic peptide solutions prepared likewise were adjusted in pH or NaCl concentration and then sonicated and temperature-annealed as indicated above.

Epifluorescence microscopy. 10 µL of cyclic peptide samples annealed in presence of 10 µM thioflavin-T (*vide supra*) were deposited on glass slides and left to dry completely overnight in the dark at room temperature before imaging (Ex=475/35 nm; Em=530/43 nm).

Scanning-transmission electron microscopy (STEM). Annealed nanosheet samples were diluted 10-fold with water and 4 µL spotted on Cu grids. Once dry, samples were imaged without washing nor staining.

Atomic force microscopy (AFM). Annealed nanosheet samples were concentrated by centrifugation (10 krcf/10 min), resuspending the pellet in

water by gentle pipetting using a tenth of its original volume. 5 µL of this 10-fold concentrated sample were spotted on mica, left to dry, and imaged by non-contact mode AFM.

Note. Neither STEM nor AFM samples contain thioflavin-T.

Full details on the synthetic procedures and experimental protocols can be found in the electronic supporting information in: https://chemistry-europe.onlinelibrary.wiley.com

Acknowledgements

This work was partially supported by the Spanish Agencia Estatal de Investigación (AEI) [SAF2017-89890-R], Xunta de Galicia (ED431C 2017/25, 2016-AD031 and ED431G/09) and the European Commission (EC) (European Regional Development Fund – ERDF). I.I. thanks the EC and AEI for MSCA-IF (2018-843332) and Juan de la Cierva (FJCI-2017-31795) fellowships, respectively. J.M. thanks the Ramón y Cajal (RYC-2013-13784), an ISCIII (COV20/00297), the ERC-Stg (DYNAP-677786), the ERC-PoC (TraffikGene, 838002), and a Young Investigator Grant from the HFSP (RGY0066/2017).

Keywords: Supramolecular Chemistry • Self-assembly • nanosheet • 2D • nanotube

[1] B. Shen, Y. Kim, M. Lee, *Adv. Mater.* **2020**, 1905669.
[2] J. Zhu, C. Yang, C. Lu, F. Zhang, Z. Yuan, X. Zhuang, *Acc. Chem. Res.* **2018**, *51*, 3191–3202.
[3] R. Dong, T. Zhang, X. Feng, *Chem. Rev.* **2018**, *118*, 6189–6235.
[4] C. Tan, X. Cao, X.-J. Wu, Q. He, J. Yang, X. Zhang, J. Chen, W. Zhao, S. Han, G.-H. Nam, M. Sindoro, H. Zhang, *Chem. Rev.* **2017**, *117*, 6225–6331.
[5] S. Cai, W. Zhang, R. N. Zuckermann, Z. Li, X. Zhao, Y. Liu, *Adv. Mater.* **2015**, *27*, 5762–5770.
[6] J. del Barrio, J. Liu, R. A. Brady, C. S. Y. Tan, S. Chiodini, M. Ricci, R. Fernández-Leiro, C.-J. Tsai, P. Vasileiadi, L. D. Michele, D. Lairez, C. Toprakcioglu, O. A. Scherman, *J. Am. Chem. Soc.* **2019**, *141*, 14021–14025.
[7] Q. Zhang, R.-J. Xing, W.-Z. Wang, Y.-X. Deng, D.-H. Qu, H. Tian, *iScience* **2019**, *19*, 14–24.
[8] H. Liu, Z. Zhang, Y. Zhao, Y. Zhou, B. Xue, Y. Han, Y. Wang, X. Mu, S. Zang, X. Zhou, Z. Li, *J. Mater. Chem. B* **2019**, *7*, 1435–1441.
[9] Y. Li, C. Qin, Q. Li, P. Wang, X. Miao, H. Jin, W. Ao, L. Cao, *Adv. Opt. Mater.* **2020**, 1902154.
[10] K. C. Bentz, S. M. Cohen, *Angew. Chem. Int. Ed.* **2018**, *57*, 14992–15001.
[11] Y. Ding, M. Cai, Z. Cui, L. Huang, L. Wang, X. Lu, Y. Cai, *Angew. Chem. Int. Ed.* **2018**, *57*, 1053–1056.
[12] X. He, Y. He, M.-S. Hsiao, R. L. Harniman, S. Pearce, M. A. Winnik, I. Manners, *J. Am. Chem. Soc.* **2017**, *139*, 9221–9228.
[13] X. He, M.-S. Hsiao, C. E. Boott, R. L. Harniman, A. Nazemi, X. Li, M. A. Winnik, I. Manners, *Nat. Mater.* **2017**, *16*, 481–488.
[14] J. Xu, G. Wu, Z. Wang, X. Zhang, *Chem. Sci.* **2012**, *3*, 3227–3230.
[15] B. Sun, Y. Kim, Y. Wang, H. Wang, J. Kim, X. Liu, M. Lee, *Nat. Mater.* **2018**, *17*, 599–604.
[16] X. Liu, X. Zhou, B. Shen, Y. Kim, H. Wang, W. Pan, J. Kim, M. Lee, *J. Am. Chem. Soc.* **2020**, *142*, 1904–1910.
[17] T. Fukui, S. Kawai, S. Fujinuma, Y. Matsushita, T. Yasuda, T. Sakurai, S. Seki, M. Takeuchi, K. Sugiyasu, *Nat. Chem.* **2017**, *9*, 493–499.
[18] M. Inam, G. Cambridge, A. Pitto-Barry, Z. P. L. Laker, N. R. Wilson, R. T. Mathers, A. P. Dove, R. K. O'Reilly, *Chem. Sci.* **2017**, *8*, 4223–4230.
[19] B. A. G. Lamers, R. Graf, B. F. M. de Waal, G. Vantomme, A. R. A. Palmans, E. W. Meijer, *J. Am. Chem. Soc.* **2019**, *141*, 15456–15463.
[20] C. E. Boott, A. Nazemi, I. Manners, *Angew. Chem. Int. Ed.* **2015**, *54*, 13876–13894.
[21] H. Zhang, *ACS Nano* **2015**, *9*, 9451–9469.
[22] A. M. Evans, L. R. Parent, N. C. Flanders, R. P. Bisbey, E. Vitaku, M. S. Kirschner, R. D. Schaller, L. X. Chen, N. C. Gianneschi, W. R. Dichtel, *Science* **2018**, *361*, 52–57.
[23] J. W. Colson, W. R. Dichtel, *Nat. Chem.* **2013**, *5*, 453–465.
[24] I. Insua, J. Montenegro, *Chem* **2020**, *6*, 1652–1682.
[25] H. Jun, F. Zhang, T. Shepherd, S. Ratanalert, X. Qi, H. Yan, M. Bathe, *Sci. Adv.* **2019**, *5*, eaav0655.
[26] E. D. Santis, M. G. Ryadnov, *Chem. Soc. Rev.* **2015**, *44*, 8288–8300.
[27] J. Wang, K. Liu, R. Xing, X. Yan, *Chem. Soc. Rev.* **2016**, *45*, 5589–5604.
[28] K. Sato, M. P. Hendricks, L. C. Palmer, S. I. Stupp, *Chem. Soc. Rev.* **2018**, *47*, 7539–7551.
[29] A. Lampel, *Chem* **2020**, *6*, 1222–1236.
[30] T. O. Omosun, M.-C. Hsieh, W. S. Childers, D. Das, A. K. Mehta, N. R. Anthony, T. Pan, M. A. Grover, K. M. Berland, D. G. Lynn, *Nat. Chem.* **2017**, *9*, 805–809.
[31] H. Zhu, H. Wang, B. Shi, L. Shangguan, W. Tong, G. Yu, Z. Mao, F. Huang, *Nat. Commun.* **2019**, *10*, 2412.
[32] A. Sorrenti, J. Leira-Iglesias, A. Sato, T. M. Hermans, *Nat. Commun.* **2017**, *8*, 15899.
[33] W. Bai, C. J. Sargent, J.-M. Choi, R. V. Pappu, F. Zhang, *Nat. Commun.* **2019**, *10*, 3317.
[34] L. Zheng, H. Zhao, Y. Han, H. Qian, L. Vukovic, J. Mecinović, P. Král, W. T. S. Huck, *Nat. Chem.* **2019**, *11*, 359–366.
[35] W. Zhang, P. Yang, *Adv. Compos. Hybrid. Mater.* **2019**, *2*, 201–213.
[36] L. Liu, L. H. Klausen, M. Dong, *Nano Today* **2018**, *23*, 40–58.
[37] Y. Lin, M. R. Thomas, A. Gelmi, V. Leonardo, E. T. Pashuck, S. A. Maynard, Y. Wang, M. M. Stevens, *J. Am. Chem. Soc.* **2017**, *139*, 13592–13595.
[38] U. Lewandowska, W. Zajaczkowski, S. Corra, J. Tanabe, R. Borrmann, E. M. Benetti, S. Stappert, K. Watanabe, N. A. K. Ochs, R. Schaeublin, C. Li, E. Yashima, W. Pisula, K. Müllen, H. Wennemers, *Nat. Chem.* **2017**, *9*, 1068–1072.
[39] A. D. Merg, G. Touponse, E. van Genderen, X. Zuo, A. Bazrafshan, T. Blum, S. Hughes, K. Salaita, J. P. Abrahams, V. P. Conticello, *Angew. Chem. Int. Ed.* **2019**, *58*, 13507–13512.
[40] J. D. Brodin, J. R. Carr, P. A. Sontz, F. A. Tezcan, *Proc. Natl. Acad. Sci. USA* **2014**, *111*, 2897–2902.
[41] K. T. Nam, S. A. Shelby, P. H. Choi, A. B. Marciel, R. Chen, L. Tan, T. K. Chu, R. A. Mesch, B.-C. Lee, M. D. Connolly, C. Kisielowski, R. N. Zuckermann, *Nat. Mater.* **2010**, *9*, 454–460.
[42] Y. Lin, M. Penna, M. R. Thomas, J. P. Wojciechowski, V. Leonardo, Y. Wang, E. T. Pashuck, I. Yarovsky, M. M. Stevens, *ACS Nano* **2019**, *13*, 1900–1909.
[43] E. L. Magnotti, S. A. Hughes, R. S. Dillard, S. Wang, L. Hough, A. Karumbamkandathil, T. Lian, J. S. Wall, X. Zuo, E. R. Wright, V. P. Conticello, *J. Am. Chem. Soc.* **2016**, *138*, 16274–16282.
[44] T. Jiang, E. L. Magnotti, V. P. Conticello, *Interface Focus* **2017**, *7*, 20160141.
[45] T. Jiang, C. Xu, X. Zuo, V. P. Conticello, *Angew. Chem. Int. Ed.* **2014**, *53*, 8367–8371.
[46] A. D. Merg, E. van Genderen, A. Bazrafshan, H. Su, X. Zuo, G. Touponse, T. B. Blum, K. Salaita, J. P. Abrahams, V. P. Conticello, *J. Am. Chem. Soc.* **2019**, *141*, 20107–20117.
[47] A. Battigelli, J. H. Kim, D. C. Dehigaspitiya, C. Proulx, E. J. Robertson, D. J. Murray, B. Rad, K. Kirshenbaum, R. N. Zuckermann, *ACS Nano* **2018**, *12*, 2455–2465.
[48] R. M. Capito, H. S. Azevedo, Y. S. Velichko, A. Mata, S. I. Stupp, *Science* **2008**, *319*, 1812–1816.
[49] X. Jia, K. Minami, K. Uto, A. C. Chang, J. P. Hill, T. Ueki, J. Nakanishi, K. Ariga, *Small* **2019**, *15*, 1804640.
[50] B. Rubinov, N. Wagner, M. Matmor, O. Regev, N. Ashkenasy, G. Ashkenasy, *ACS Nano* **2012**, *6*, 7893–7901.
[51] W. Wei, Y. Liu, N. Xiong, L. Yu, T. Zhang, H. Song, F. Tang, *ChemPlusChem* **2019**, *84*, 374–381.
[52] S. Zhang, T. Holmes, C. Lockshin, A. Rich, *Proc. Natl. Acad. Sci. USA* **1993**, *90*, 3334–3338.
[53] K. Lu, J. Jacob, P. Thiyagarajan, V. P. Conticello, D. G. Lynn, *J. Am. Chem. Soc.* **2003**, *125*, 6391–6393.

[54] M. R. Ghadiri, J. R. Granja, R. A. Milligan, D. E. McRee, N. Khazanovich, *Nature* **1993**, *366*, 324–327.
[55] M. R. Silk, J. Newman, J. C. Ratcliffe, J. F. White, T. Caradoc-Davies, J. R. Price, S. Perrier, P. E. Thompson, D. K. Chalmers, *Chem. Commun.* **2017**, *53*, 6613–6616.
[56] J. Montenegro, M. R. Ghadiri, J. R. Granja, *Acc. Chem. Res.* **2013**, *46*, 2955–2965.
[57] A. Fuertes, M. Juanes, J. R. Granja, J. Montenegro, *Chem. Commun.* **2017**, *53*, 7861–7871.
[58] A. Méndez-Ardoy, J. R. Granja, J. Montenegro, *Nanoscale Horiz.* **2018**, *3*, 391–396.
[59] A. Mendez-Ardoy, A. Bayón-Fernández, Z. Yu, C. Abell, J. R. Granja, J. Montenegro, *Angew. Chem. Int. Ed.* **2020**, *132*, 6969–6975.
[60] M. Hartlieb, S. Catrouillet, A. Kuroki, C. Sanchez-Cano, R. Peltier, S. Perrier, *Chem. Sci.* **2019**, *10*, 5476–5483.
[61] J. C. Brendel, J. Sanchis, S. Catrouillet, E. Czuba, M. Z. Chen, B. M. Long, C. Nowell, A. Johnston, K. A. Jolliffe, S. Perrier, *Angew. Chem.* **2018**, *130*, 16920–16924.
[62] I. Insua, J. Montenegro, *J. Am. Chem. Soc.* **2020**, *142*, 300–307.
[63] L. S. Wolfe, M. F. Calabrese, A. Nath, D. V. Blaho, A. D. Miranker, Y. Xiong, *Proc. Natl. Acad. Sci. USA* **2010**, *107*, 16863–16868.

Entry for the Table of Contents

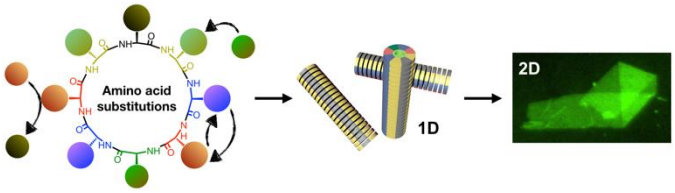

Two-dimensional (2D) supramolecular materials combine the responsiveness of non-covalent systems with the capacities of high surface materials. Hierarchical peptide self-assembly provides a powerful platform for the nanofabrication of new biocompatible 2D architectures. We describe here the structure-assembly relationships of a cyclic octapeptide capable of sequentially assembling one-dimensional (1D) nanotubes and 2D nanosheets in aqueous environment.

Institute and/or researcher Twitter usernames: @ciqususc, @InsuaNacho, @MontenegroLabo